Sensors and Materials, Vol. 31, No. 4 (2019) 1281–1287
MYU Tokyo

S & M 1855

Dopant Concentration Dependence of Luminescence in Cu-doped Lithium Aluminophosphate Glasses

Daiki Shiratori,* Yuya Isokawa, Noriaki Kawaguchi, and Takayuki Yanagida

Nara Institute of Science and Technology, 8916-5 Takayama-cho, Ikoma, Nara, 630-0192, Japan

(Received November 29, 2018; accepted April 2, 2019)

Keywords: glass, copper, phosphate, scintillation, luminescence

We have prepared glasses with the composition of Cu-doped $30Li_3PO_4$-$70Al(PO_3)_3$ and investigated their luminescence characteristics. The glass samples were synthesized by the melt quenching method, and the Cu concentrations of the prepared samples were 0.1, 0.2, 0.5, and 1.0%. In the absorption spectrum, the absorptions due to Cu^+ and Cu^{2+} around 290 and 850 nm were observed, respectively. The absorption due to Cu^{2+} increased in proportion to the amount of Cu. In the photoluminescence (PL) decay curve, the PL decay time was a typical value of the $3d^94s^1$–$3d^{10}$ transition of Cu^+ (~30 μs). The scintillation spectra showed a broad emission band from 400 to 600 nm, and the emission intensities were proportional to the Cu concentration.

1. Introduction

Fluorescent materials have been used in personal dose monitoring devices,[1] radiation detectors for medical purposes such a PET or CT imaging,[2] environmental monitoring,[3] security,[4] oil logging,[5] and high-energy physics. The emission intensity induced by ionizing radiation is proportional to the energy deposited in the material by the interaction between the ionizing radiation and the material, and we can estimate the radiation dose or energy from the luminescence intensity. When the luminescence material is irradiated by ionizing radiation, firstly, an energetic electron is ejected from the atom and generates a large number of secondary electrons via an interaction such as Coulomb scattering. These secondary electrons immediately show light emission if they recombine with holes at localized luminescence centers, and such an immediate emission is called scintillation. As an emission center in a phosphor, rare-earth elements such as Ce or Eu are frequently used. Rare-earth elements are industrially essential and are important for luminescence in the visible and NIR ranges in phosphors. Recently, the stable supply of rare-earth elements has become a big problem, and rare-earth-free materials have attracted much attention. For such purpose, transition metal ions are one of the solutions since some of them can show efficient luminescence mainly due to 3d–3d transitions. Among them, the $3d^{10}$–$4s3d^9$ transition of Cu^+ shows luminescence in the blue to green regions.[8–11] The luminescence wavelength of Cu^+ is suitable for the wavelength sensitivity of conventional photomultiplier tubes (PMTs), and it is a preferable property for radiation detectors. Therefore, we have focused on Cu ion as a dopant of luminescence materials.

*Corresponding author: e-mail: shiratori.daiki.sc3@ms.naist.jp
https://doi.org/10.18494/SAM.2019.2188

ISSN 0914-4935 © MYU K.K.

Currently, from the viewpoint of material forms, only two kinds of glass materials, $NaPO_3$-$Al(PO_3)_3$ glass for dosimeters[12] and Li glass for scintillation detectors,[13] are used in the field of radiation measurements. Therefore, there is room for the study of glass materials in radiation measurements.

In this work, we focus on Li_3PO_4-$Al(PO_3)_3$ glass, which has a lower effective atomic number (Z_{eff}) of 11.9, and it is lighter than the commercial Ag-doped $NaPO_3$-$Al(PO_3)_3$ glass (Z_{eff} = 12.4) for dosimeters provided by Chiyoda Technol Corp. Our group has reported on the addition of Ce or Ag to Li_3PO_4-$Al(PO_3)_3$ glasses so far and investigated the emission characteristics by irradiation with ionizing radiation.[14,15] Here, Cu was selected as the luminescence center for the reason mentioned earlier, and we investigated the photoluminescence (PL) and X-ray-induced scintillation properties of Cu-doped Li_3PO_4-$Al(PO_3)_3$ glasses.

2. Materials and Methods

2.1 Sample preparation

Cu-doped Li_3PO_4-$Al(PO_3)_3$ glasses were prepared by a conventional melt-quenching method. The raw material of Cu_2O (2N) was used as a dopant, and 0.1, 0.2, 0.5, and 1.0% were added with respect to the host. The starting materials of Li_3PO_4 (4N) and $Al(PO_3)_3$ (4N) were homogeneously mixed in a ratio of 30:70, respectively, and the mixture was then melted inside an alumina crucible using an electric furnace at 1300 ℃ for 30 min in an ambient atmosphere. The melt was press-quenched with preheated stainless-steel plates kept at about 200 ℃. After cooling the glass sufficiently, we cut and polished the samples to the thickness of 1.29 ± 0.25 mm and the typical size of ~7 × 7 mm^2. The prepared glass samples were evaluated by the following experiments.

2.2 Evaluation of optical and X-ray-induced scintillation properties

The optical absorption spectra were obtained using a spectrophotometer (V670, JASCO) across a spectral range from 190 to 2700 nm. The measuring wavelength interval was 1 nm. The PL excitation/emission spectra and PL quantum yields (QYs) were measured using Quantaurus-QY (C11347, Hamamatsu Photonics). The monitoring excitation and emission wavelength ranges were from 250 to 500 nm and 200 to 950 nm, respectively, with 10 nm intervals. The PL decay curves were evaluated using a fluorescence lifetime measurement system Quantaurus-Tau (C11367, Hamamatsu Photonics). The excitation and monitoring wavelengths were determined on the basis of the measured PL excitation/emission contour graph.

Scintillation spectra were evaluated at room temperature using our laboratory-made setup.[16] An X-ray generator (OURTEX Corporation) equipped with a conventional X-ray tube was used as the radiation source to measure the scintillation spectrum. The X-ray tube was operated with a tube voltage and current of 40 kV and 1.2 mA, respectively. The emission generated

by irradiating X-ray was guided through an optical fiber to a monochromator equipped with a CCD-based detector (Shamrock 163 monochromator and Andor DU-420-BU2 CCD) to obtain a spectrum. The scintillation decay time profiles were measured using a custom-made system available from Hamamatsu Photonics. This system enabled us to measure the X-ray-induced scintillation decay curve by the time-correlated single-photon counting (TCSPC) technique.[17]

3. Results and Discussion

3.1 Samples and absorption spectra

Figure 1 shows photographs of Cu-doped Li_3PO_4-$Al(PO_3)_3$ glasses under (a) room light and (b) irradiated by UV lamp (302 nm). All prepared glasses were transparent to the naked eyes under room light. A previous study clarified that the undoped sample was transparent from visible to NIR wavelengths,[15] and Cu doping caused a clear coloration. We confirmed by the naked eyes that the samples became blue in color with increasing Cu concentration. From the visual observation, we did not see a clear dependence of luminescence intensity on the Cu concentration when we irradiated UV photons.

Figure 2 indicates the absorption spectra of the glass samples. The absorption spectra indicate a broad absorption band from 600 to 1300 nm. The blue coloring of the samples with the increase in Cu concentration is due to this absorption of red color, and the origin of this absorption band would be attributed to Cu^{2+}.[8] According to the transmittance spectra of the undoped Li_3PO_4-$Al(PO_3)_3$ reported previously, the absorption edge appeared at ~240 nm (5.2 eV). In the Cu-doped Li_3PO_4-$Al(PO_3)_3$ glasses, we observed the absorption bands in a shorter wavelength of around 290 nm, and this absorption band is due to the $3d^{10}$–$4s3d^9$ transition of Cu^+ ions.

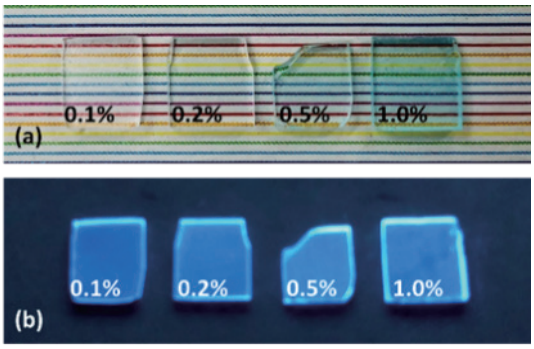

Fig. 1. (Color online) Photographs of the glass samples under (a) room light and (b) UV irradiation (302 nm).

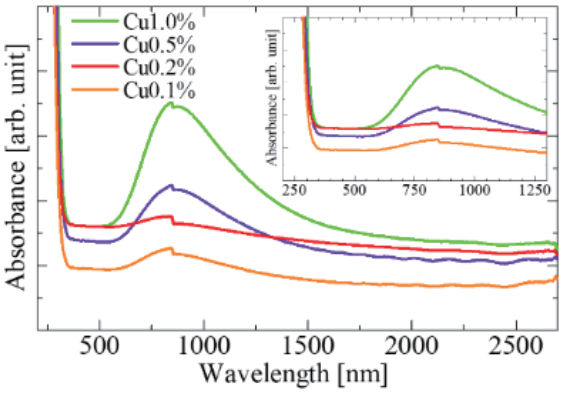

Fig. 2. (Color online) Room-temperature optical absorbance spectra of Cu-doped glasses in the 190–2700 nm range. Inset expands the spectra from UV to NIR ranges.

3.2 PL properties

A PL excitation/emission map of the Cu 1.0%-doped glass sample is shown in Fig. 3. All samples had a similar spectral shape characterized by one emission band excited from 270 to 290 nm, which well coincided with the absorption band shown in Fig. 2. The emission wavelength is near 450 nm, and the emission origin is ascribed to the $3d^9 4s^1$–$3d^{10}$ transitions of Cu^+ ions. The inset of Fig. 3 shows the fitting result of PL spectra excited with 275 nm of Cu 1.0%-doped glass sample by a single Gaussian approximation. The spectrum can be clearly reproduced by a single Gaussian function. By focusing on this emission band, we evaluated the PL QYs. As a result, the obtained QYs were 2–4%. In the QYs, we could not confirm the dependence of QYs on the concentration of Cu since the typical error of this measurement was ±2%.

Figure 4 shows PL decay curves of Cu-doped glasses. The excitation and monitoring wavelengths were 275 and 460 nm, respectively. The decay times were deduced by an approximation of a single exponential function. The obtained decay time constants were 24.5–25.4 μs, and these were close to the typical decay time constants of Cu^+-doped materials reported previously.[9] Except for the 1.0% Cu sample, the decay time increased with increasing Cu concentration.

In the case of some of the Cu-doped crystalline materials, Cu^+ ions can show different PL characteristics when they occupy different sites. Such an emission feature is caused by the difference in the crystal field, and it especially depends on the oxygen coordination number in oxide materials. A similar phenomenon is also observed in glass materials, and in the case of Cu-doped SiO_2, the six-coordinated-like Cu^+ gives rise to PL emission at 490–500 nm whereas the eight-coordinated-like Cu^+ shows PL around 430 nm when excited with UV light.[11] In our case, the PL peak appeared around 450 nm. Although we cannot define clearly the coordinated number in amorphous materials, the luminescence of the present samples would be considered owing to emission from the eight-coordinated-like Cu^+. Despite the clear detection of Cu^{2+} in the absorption spectra, we did not observe an emission relating to Cu^{2+}.

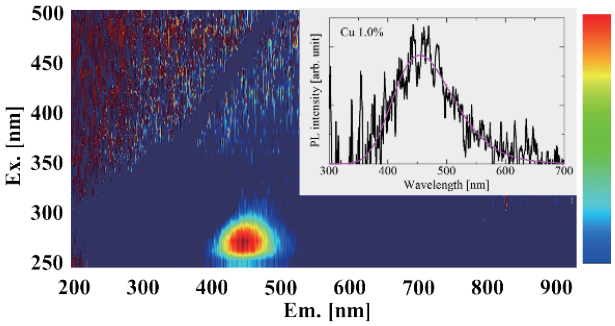

Fig. 3. (Color online) PL excitation/emission map of the 1.0% Cu-doped glass sample. The vertical and horizontal axes represent the excitation and emission wavelengths, respectively. Inset is the PL spectrum of a Cu 1.0%-doped glass sample deconvoluted by a single Gaussian.

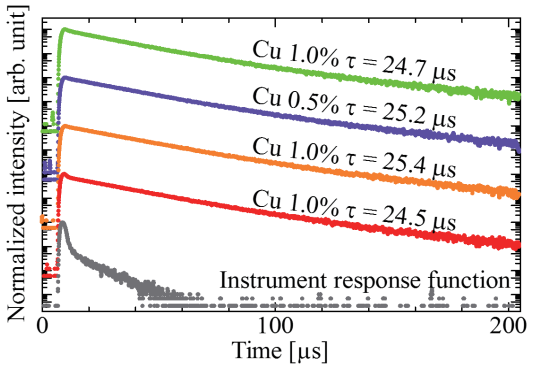

Fig. 4. (Color online) PL decay profiles of glass samples. The monitoring wavelength is 460 nm, and the excitation wavelength is 275 nm.

3.3 Scintillation characterizations

Figure 5 exhibits X-ray-induced scintillation spectra of Cu-doped glass samples. A broad emission was confirmed from 400 to 600 nm, and the spectral shape was similar to that of PL, although the scintillation showed a broader spectral feature than PL. Although the intensity of the scintillation spectrum is generally a qualitative value, we can roughly compare the emission intensities among the samples since the sizes and Z_{eff} of the samples were similar. Among the present samples, Cu 0.5- and 1%-doped samples exhibited the highest emission intensity, and the optimum Cu dopant concentration of this glass was around 0.5–1.0%. To consider the reason for the spectrum broadness of scintillation, we have conducted a double Gaussian fitting to the emission spectrum of the Cu 1.0%-doped sample. Figure 6 shows the deconvolution result of the Cu 1.0%-doped sample. The spectrum can be deconvoluted to a sum of two Gaussians. The short-wavelength component had a peak around 450 nm, and the spectral shape resembled the emission band observed in PL. Therefore, we can consider that the wider spectral shape of scintillation could be attributed to the emergence of a new emission peak at 502 nm. As discussed in PL, Cu^+ is known to show different emission bands depending on the oxygen coordinate environment including the possibility of a Cu^+–Cu^+ dimer,[18] and the marginal emission from Cu^+ at different environments would be observed in the scintillation spectrum that causes the broad spectral feature.

X-ray-induced scintillation decay time profiles of all the glasses are indicated in Fig. 7. The decay curves were approximated by a sum of two exponential decay functions, neglecting the spikelike component at the rise part since it was due to the instrumental response. The obtained decay times are summarized in Table 1. The obtained decay time constants of the second component were similar to those in PL. Therefore, it can be inferred that the origin of this decay time constant would be due to $3d^9 4s^1$–$3d^{10}$ transitions of Cu^+. On the other hand, the relatively fast decay time constant of a few microseconds would be due to the long-wavelength component peaking at 502 nm confirmed in scintillation (Fig. 6) since our equipment could not resolve the wavelength. From the spectral shapes and decay times, it would be reasonable that the emissions due to Cu^+ at different oxygen coordinate environments or Cu^+–Cu^+ dimer appeared in scintillation.[18] In order to clarify the origin of the above-mentioned emission, additional verification experiments are required.

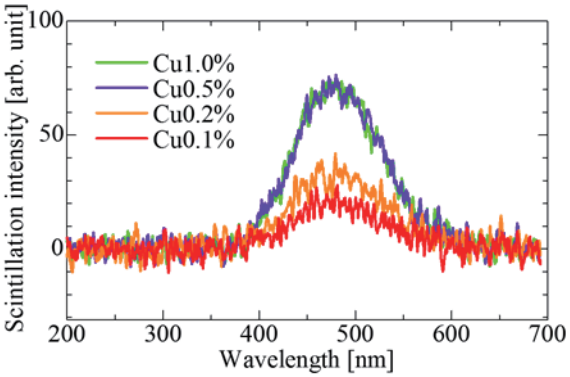

Fig. 5. (Color online) X-ray-induced scintillation properties of Cu-doped glass samples.

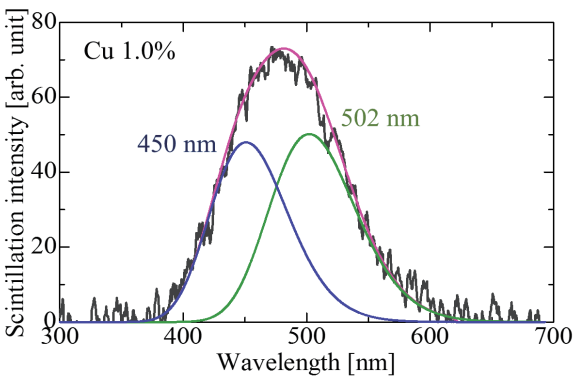

Fig. 6 (Color online) Scintillation spectrum of Cu 1.0%-doped sample deconvoluted by double Gaussian.

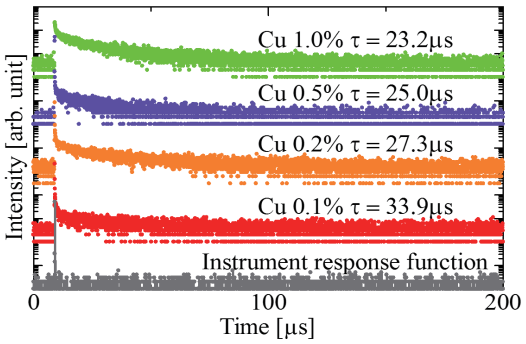

Fig. 7. (Color online) X-ray-induced scintillation decay profiles of glasses.

Table 1
RL decay time constants as a function of Cu concentration.

Cu concentration (%)	Decay time constants (μs)	
	1st	2nd
0.1	1.01	33.0
0.2	2.11	27.3
0.5	1.26	25.0
1.0	1.59	23.2

4. Conclusion

Cu-doped $30Li_3PO_4$-$70Al(PO_3)_3$ glasses were synthesized by the melt quenching method. The synthesized samples were evaluated in terms of their optical, PL, and scintillation properties. When the concentration of Cu increased, the samples showed a coloration, and the Cu 1.0%-doped glass sample revealed the blue color as seen by the naked eye. In PL and scintillation, the luminescence by Cu^+ was confirmed. The emission due to Cu^{2+} is observed only in the scintillation. However, from comparisons on the fluorescence QY and scintillation intensity of the present samples with other materials, some improvements such as adjusting the composition of the host metal or introducing coadditives will be necessary. With regard to emission at 502 nm in scintillation, it would be necessary to investigate its emission origin by vacuum ultraviolet (VUV) light excitation excitation and local electronic state analysis.

Acknowledgments

This work was supported by Grants-in-Aid for Scientific Research (A) (17H01375) and (B) (18H03468) from the Ministry of Education, Culture, Sports, Science and Technology of the Japanese government (MEXT) and A-STEP from the Japan Science and Technology Agency (JST). The Cooperative Research Project of the Research Institute of Electronics, Shizuoka University, Terumo Foundation for Life Sciences and Arts, Izumi Science and Technology Foundation, The Kazuchika Okura Memorial Foundation, and The Iwatani Naoji Foundation are also acknowledged.

References

1 Y. Miyamoto, H. Nanto, T. Kurobori, Y. Fujimoto, T. Yanagida, J. Ueda, S. Tanabe, and T. Yamamoto: Radiat. Meas. **71** (2014) 529.
2 T. Yanagida, A. Yoshikawa, Y. Yokota, K. Kamada, Y. Usuki, S. Yamamoto, M. Miyake, M. Baba, K. Kumagai, K. Sasaki, M. Ito, N. Abe, Y. Fujimoto, S. Maeo, Y. Furuya, H. Tanaka, A. Fukabori, T. Rodrigues dos Santos, M. Takeda, and N. Ohuchi: IEEE Trans. Nucl. Sci. **57** (2010) 1492.
3 K. Watanabe, T. Yanagida, and K. Fukuda: Sens. Mater. **27** (2015) 1.
4 D. Totsuka, T. Yanagida, K. Fukuda, N. Kawaguchi, Y. Fujimoto, J. Pejchal, Y. Yokota, and A. Yoshikawa: Nucl. Instrum. Methods Phys. Res., Sect. A **659** (2011) 399.

5 T. Yanagida, Y. Fujimoto, S. Kurosawa, K. Kamada, H. Takahashi, Y. Fukazawa, M. Nikl, and V. Chani: Jpn. J. Appl. Phys. **52** (2013) 076401.
6 H. Takahashi, T. Yanagida, D. Kasama, T. Ito, M. Kokubun, K. Makishima, T. Yanagitani, H. Yagi, T. Shigeta, and T. Ito: IEEE Trans. Nucl. Sci. **53** (2006) 2404.
7 T. Itoh, M. Kokubun, T. Takashima, T. Honda, K. Makishima, T. Tanaka, T. Yanagida, S. Hirakuri, R. Miyawaki, H. Takahashi, K. Nakazawa, and T. Takahashi: IEEE Trans. Nucl. Sci. **53** (2006) 2983.
8 S. Gómez, I. Urra, R. Valiente, and F. Rodríguez: Sol. Energy Mater. Sol. Cells **95** (2011) 2018.
9 B. Tiwari, N. S. Rawat, D. G. Desai, S. G. Singh, M. Tyagi, P. Ratna, S. C. Gadkari, and M. S. Kulkarni: J. Lumin. **130** (2010) 2076.
10 Q. Zhang, G. Chen, G. Dong, G. Zhang, X. Liu, J. Qiu, Q. Zhou, Q. Chen, and D. Chen: Chem. Phys. Lett. **482** (2009) 228.
11 E. Borsella, A. Dal Vecchio, M. A. Garcìa, C. Sada, F. Gonella, R. Polloni, A. Quaranta, and L. J. G. W. van Wilderen: J. Appl. Phys. **91** (2002) 90.
12 Y. Miyamoto, T. Yamamoto, K. Kinoshita, S. Koyama, Y. Takei, H. Nanto, Y. Shimotsuma, M. Sakakura, K. Miura, and K. Hirao: Radiat. Meas. **45** (2010) 546.
13 T. Yanagida, N. Kawaguchi, Y. Fujimoto, K. Fukuda, Y. Yokota, A. Yamazaki, K. Watanabe, J. Pejchal, A. Uritani, T. Iguchi, and A. Yoshikawa: Opt. Mater. **33** (2011) 1243.
14 H. Tatsumi, G. Okada, T. Yanagida, and H. Masai: Chem. Lett. **45** (2016) 280.
15 H. Tatsumi, G. Okada, T. Yanagida, and H. Masai: J. Ceram. Soc. Jpn. **124** (2016) 550.
16 T. Yanagida, K. Kamada, Y. Fujimoto, H. Yagi, and T. Yanagitani: Opt. Mater. **35** (2013) 2480.
17 T. Yanagida, Y. Fujimoto, T. Ito, K. Uchiyama, and K. Mori: Appl. Phys. Express **7** (2014) 4.
18 H. Ikeda, T. Murata, and S. Fujino: Mater. Chem. Phys. **162** (2015) 431.